

Comparing the performance of direct and parametric drives for piezoelectric MEMS actuators

Samer Houri* and Veronique Rochus

imec, Leuven, Belgium

(Dated: May 6, 2025)

This work investigates and compares the response of piezoelectrically actuated nonlinear micro-electromechanical devices (MEMS) to direct and to degenerate parametric drives. We describe the regime of degenerate parametric amplification in piezoelectric Duffing-type nonlinear MEMS devices using a single mode expansion, we then explore the existence of regions in parameter space where parametric excitation maybe advantageous compared to direct drive, which we label “parametric advantage”. Analytical, experimental, and numerical verification demonstrates that parametric advantage can not exist if both pump and signal voltages are accounted for in the total voltage budget. This work determines non-dimensional scaling rules that can act as guidelines for selecting an optimal operating regime for degenerate parametric amplification.

The description of parametric amplification in atomic force microscope cantilever by Rugar et al. [1] was the first to demonstrate amplification and noise squeezing in a microelectromechanical device (MEMS). Furthermore, the authors established a simplified analytical expression for parametric amplification in a linear MEMS device, which relates the parametric gain to the quality factor and the parametric modulation depth. Thereafter, several demonstrations of parametric amplification and oscillations followed in a large range of micro- and nano- devices including MEMS resonators [2–7], nanoelectromechanical device (NEMS) resonators [8–11], micromirrors [12, 13], sensors [14, 15], gyroscopes [16], and energy harvesters [17, 18] to name just a few.

In the case of M/NEMS devices, parametric pumping can take on an additional layer of complexity, since M/NEMS devices exhibit (typically cubic) nonlinearities, which only become more pronounced as the devices are scaled down [19, 20]. These Duffing-type nonlinearities change significantly the typical responses of parametric systems [21–26].

This work focuses on the regime of degenerate (i.e., frequency of pump = 2 x frequency of signal) parametric amplification and aims to answer the following questions; How to express the responsiveness of a nonlinear MEMS device to parametric amplification in terms of the device parameters? Furthermore, given a voltage constrained operation, when does the parametric amplification regime become advantageous compared to directly forcing the system? And how does this “parametric advantage” depend on the intrinsic properties, including nonlinearity, of typical M/NEMS resonators?

The concept of parametric advantage is represented schematically in Fig. 1. A typical resonance mode of a MEMS device, represented by a lumped spring-mass system, is driven via a harmonic force. As this direct forcing is increased the amplitude of the resonator increases, as shown in the figure, for simplicity only the

linear case is shown. However, it is equally possible to increase the amplitude of the resonator by periodically tuning the spring’s stiffness at twice the drive frequency (i.e., parametric pumping) where the response of the resonator to a small driving force becomes amplified, with the amplification factor increasing asymptotically as the modulation strength approaches the threshold of instability. At a given point the response of the parametrically pumped resonator overtakes that of direct forcing, we label this region “parametric advantage” and define it as the region in parameter space where the response of the resonator to parametric amplification exceeds the response of the resonator to direct forcing at the same overall voltage. If one does not account for the parametric pump in the overall voltage budget, then parametric amplification would be purely advantageous and we obtain the typical parametric gain expressions [1, 23]. This traditional approach does not account for the pump voltage in its gain calculations whereas in many examples of sensors and actuators the overall voltage is largely constrained.

To analytically identify the response of a MEMS device to parametric pumping as a function of device parameters and identify whether regions of parametric advantage exists, a single mode equation of motion is used [1], note that if higher-order modes overlap the pump frequency then a multi-mode treatment of the system becomes necessary [27]. Thus, the single degree-of-freedom equation of motion is expressed as

$$\ddot{x} + \gamma\dot{x} + \omega_0^2 x + \beta x^2 + \alpha x^3 = F(t) \quad (1)$$

where x is the modal displacement, and γ , ω_0 , β , α are respectively the modal linear damping, natural frequency, quadratic and cubic (Duffing) nonlinearities, and $F(t)$ is the driving force combining direct and parametric terms. Note that the resonator is considered to be weakly damped and weakly nonlinear, a reasonable assumption for MEMS devices, therefore $(\gamma/\omega_0, \beta/\omega_0^2, \alpha/\omega_0^3) \ll 1$, and that the force term is $F(t) = \chi V(t)$ with $V(t)$ being the applied voltage and χ a linear transduction parameter in units of $(ms^{-2}V^{-1})$.

* samer.houri@imec.be

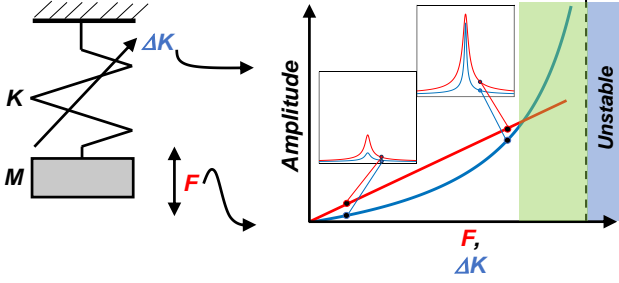


FIG. 1. Schematic representation of parametric amplification. If a linear resonator is driven via a harmonic force (F) its amplitude increases linearly with forcing (red trace). If it is parametrically pumped by modulating one of its parameters, usually the stiffness (ΔK), the amplitude increases asymptotically (blue trace). The areas of “parametric advantage” and parametric instability are shaded in green and blue, respectively. An overlay of the two plots, shown in the insets, demonstrates the narrowing of the line-widths as a function of increased parametric pumping. Note that since the x-axis is an overlay of both F and ΔK care should be taken in expressing them in the correct units.

Since the driving force contains two frequency terms, the direct drive and the parametric pumping, it can be expressed as $F(t) = F_D \cos(\omega t) + F_P \cos(2\omega t + \theta)$, where F_D is the direct drive term, F_P is the parametric pumping term, ω is the direct drive frequency, 2ω is the parametric pump frequency, and θ is any eventual phase difference between the direct and parametric voltages. It is then equally desirable to expand the displacement (x) into two frequency components such that $x = (A_1 e^{i\omega t} + A_1^* e^{-i\omega t})/2 + (A_2 e^{i2\omega t} + A_2^* e^{-i2\omega t})/2$, where the star symbol denotes complex conjugate, and A_1 and A_2 are the complex amplitudes of the 1ω and 2ω components, respectively. Furthermore, since the separation between the two frequency components is large (i.e. $= \omega$), it can be safely presumed that no chaotic response will set in [28] for reasonable forcing amplitudes.

Placing the expanded form of x in Eq. (1), and introducing a detuning parameter (δ) such that $\omega = \omega_0 \times (1 + \delta)$, gives a coupled complex-amplitude algebraic equation (see supplementary material for detailed derivation) which reads

$$\begin{cases} \left(\frac{3\bar{\alpha}}{8} (2|A_2|^2 + |A_1|^2) - \delta + i\frac{\bar{\gamma}}{2} \right) A_1 + \frac{\bar{\beta}}{2} A_2 A_1^* = \frac{\bar{F}_D}{2} \\ A_2 = -\frac{\bar{F}_P}{3} e^{i\theta} \end{cases} \quad (2)$$

Note that in Eq. (2) a steady-state solution is sought, i.e., $\dot{A}_1 = \dot{A}_2 = 0$, and that nonlinear terms in the A_2 equation are negligible. Furthermore, in Eq. (2) the parameters are expressed in a normalized form with $\bar{F}_D \rightarrow F_D/\omega_0^2$, $\bar{F}_P \rightarrow F_P/\omega_0^2$, $\bar{\chi} \rightarrow \chi/\omega_0^2$, $\bar{\gamma} \rightarrow \gamma/\omega_0$, $\bar{\alpha} \rightarrow \alpha/\omega_0^2$, and $\bar{\beta} \rightarrow \beta/\omega_0^2$.

Equation (2) demonstrates that the quadratic nonlinear term $\bar{\beta}A_2$ plays the role of parametric pump terms

in parametrically excited MEMS/NEMS resonators [1]. Therefore, no single-mode (and single degree-of-freedom) parametric pumping can take place without the presence of a quadratic nonlinear term. Furthermore, expressing the equation as a function of A_2 allows to relate the parametric pumping term (i.e., $\bar{\beta}A_2$) to the device mechanical or electromechanical properties [29, 30]. If we write $A_1 = |A_1| e^{i\phi}$ and introduce $E = |A_1|^2$, we can rewrite equation (2) in a closed form that is independent of A_2 which reads

$$\left(\frac{3\bar{\alpha}}{8} E - \delta' \right)^2 E + \left(\frac{\bar{\gamma}'}{2} \right)^2 E = \frac{\bar{F}_D^2}{4} \quad (3)$$

where $\delta' = -\frac{\bar{\alpha}\bar{F}_P^2}{4} + \delta + \frac{\bar{\beta}\bar{F}_P}{6} \cos(\theta - 2\phi)$, and $\bar{\gamma}' = \bar{\gamma} - \frac{\bar{\beta}\bar{F}_P}{3} \sin(\theta - 2\phi)$. The above equation simply states that for a sub-threshold degenerate parametric amplification of a nonlinear M/NEMS device, the system will continue to act as a Duffing type resonator [31], but with a modified detuning and damping.

Now let V_T , V_S , and V_P be the total permissible voltage, the signal voltage and the parametric pump voltage, respectively. For a voltage constrained actuator case the sum of the pump and signal voltages is limited, thus $V_T = V_S + V_P$. The condition for parametric advantage can be written down in a more rigorous form as $\eta = A_P(V_S, V_P)/A_D(V_T) \geq 1$, where A_D and A_P are the obtained amplitudes for the direct-only and parametric drive cases, respectively, and η is the ratio of the two. Note that A_D and A_P should not be confused with A_1 and A_2 , as the former pair are meant to indicate the amplitude (always around 1ω) for a system under either direct drive or parametric amplification. Whereas the latter two are meant to indicate the amplitude of the system at 1ω and 2ω respectively regardless of which excitation technique is employed.

Regions of parametric advantage correspond to the parameter space where $\eta \geq 1$ in Eq.(3). While this will be explored below, we first look at the linear case as it provides valuable insight. Without loss of generality if we consider $(\theta - 2\phi) = \pi/2$, for the case of on-resonance driving ($\delta = 0$) it is very easy to show that parametric advantage sets in when $V_T = 3\bar{\gamma}/(\bar{\chi}\bar{\beta})$. This V_T value is equivalent to the critical voltage (V_{cr}) for the onset of instability (see supplementary material). Counterintuitively, a parametric amplification advantage does not exist for linear M/NEMS when budgeting for both the signal and the pump, not below a total voltage equivalent to the threshold of instability in any case. This conclusion carries when $\delta \neq 0$ (with a different V_T value), and the introduction of a Duffing nonlinearity does not change this conclusion.

Experimentally, the results are validated using a set of flexural PZT piezoelectric disk MEMS resonators, shown in the inset of Fig. 2(a). The resonators have radii of $150 \mu\text{m}$, $200 \mu\text{m}$, and $250 \mu\text{m}$, with two devices of each diameter measured, and for the case of the

250 μm devices the second axisymmetric bending mode was equally measured. The devices consist of a stack of 6 micrometer thick layer of structural Silicon on top of which a metal-sandwiched 1 micron thick PZT layer is deposited. Before undertaking measurements, the PZT is poled and electrically stressed using 20 Vdc for a duration of an hour.

The vibration of the membranes are measured using a Polytec MSA500 laser Doppler vibrometer (LDV) in ambient conditions. An arbitrary waveform generator (KEYSIGHT 33500B) is used to generate the excitation signals which are fed into an $\times 50$ amplifier (Falco WMA-300) before being applied to the resonators via the contact pads using probes. During measurements 4 different Vdc values are applied (10, 15, 20 and 25 V) with the magnitude of the applied ac voltages such that the total voltage does not drop below zero to avoid ferroelectric depolarization [32], i.e., $V_{dc} - V_{ac} > 0$.

When measured, all devices show easily detectable resonance peaks, Fig. 2(a). The frequency sweeps are fitted to extract the main characteristics of the resonators, i.e., the resonance frequencies, quality factors, and Duffing nonlinearities, which are plotted in Fig. 2(a) through 2(c) as a function of Vdc. Whereas resonance frequencies demonstrate a near linear dependence on Vdc, the quality factor and Duffing nonlinearity do not. The drums with the smallest radius (i.e., $R = 150 \mu\text{m}$) show a negligible Duffing parameter.

By applying a weak signal to the devices at their respective resonance frequencies along with a strong 2ω voltage, parametric amplification takes place (the phase difference between the two is maintained as $\theta - 2\phi = \pi/2$). The amplitudes of vibration at 1ω and 2ω correspond to $|A_1|$ and $|A_2|$, respectively. These amplitudes are used to fit Eq. 3 and extract the value of the quadratic nonlinearity, i.e. β , as shown in the example traces in Fig. 3(a). The quadratic nonlinear parameters extracted for all the devices and bias voltages are shown in Fig. 3(b), this parameter equally does not show a strong dependence on the bias voltage.

The 150 μm devices are selected to determine experimentally the response of a linear system to parametric amplification because they lack a measurable Duffing nonlinearity. The devices are driven on resonance ($\delta = 0$) with different signal voltage levels (V_S) and a swept parametric pump amplitude (V_P). Observing the A_1 amplitude as a function of the pump voltage gives the typical parametric amplification profile, as shown in Fig. 3(c) for various drive amplitudes. The actuation and pumping voltages are kept low to avoid damaging the devices, typically below the parametric oscillation threshold (although in some measurements on various diameter devices parametric oscillation threshold was attained). An extrapolation of the direct and parametric drives demonstrates that, as predicted theoretically, the intersection of the two takes place practically upon the onset of instability, thus leaving no room for parametric advantage.

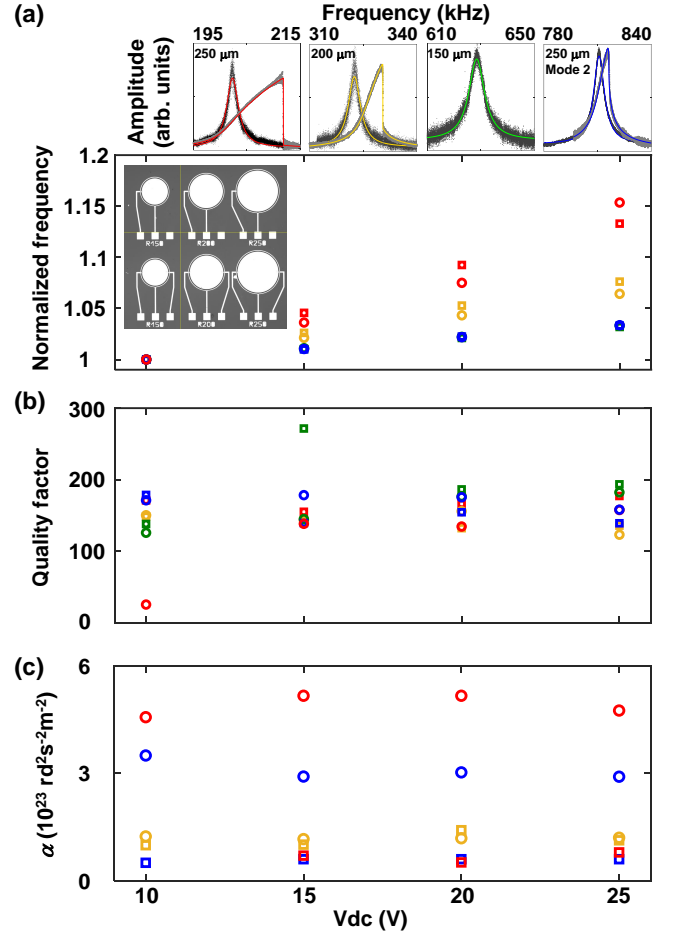


FIG. 2. Devices used and their characteristics. (a) Disks of suspended Silicon covered with a metal-sandwiched PZT and having 3 different radii (150, 200, and 250 μm) are used (shown in inset). (top panels) The linear and nonlinear resonance peaks of these devices (black dots) and their fits (colored lines) are shown as a function of decreasing diameters, with the second mode of a $R = 250 \mu\text{m}$ device shown on the rightmost plot (plots obtained for $V_{dc} = 10 \text{ V}$). The main plot shows the dependence of the modal resonance frequency on dc voltage (two devices for each diameter are used represented by the circle and the square symbols) and demonstrates a near linear dependence of the resonance frequency on V_{dc} for 250 μm (red), 200 μm (yellow), 150 μm (green), and the second mode of the 250 μm (blue), the frequency values are normalized with respect to the $V_{dc} = 10 \text{ V}$ in order for them to be visible in a single plot. (b) Quality factors as a function of dc voltage with no clear dependence on either voltage or diameter. (c) Duffing parameters as a function of V_{dc} equally showing no clear dependence.

The same conclusion can be inferred by plotting η as a function of V_S/V_T for all dc voltages, as shown in Fig. 3(d). Knowing that for $\alpha = \delta = 0$ we have $\eta = (V_S/V_T)(\bar{\gamma}/\bar{\gamma}')$ (see supplementary material), meaning that the experimental data should fall on a $y = x$ diagonal for no parametric amplification, below the diagonal for the case of de-amplification and above

the diagonal for amplification. Visibly, the bulk of the points fall near the diagonal, indicating a relatively weak parametric amplification. More importantly, the data points overwhelmingly fall below the $\eta = 1$ limit indicating no parametric advantage. Some points of the data set do cross the limit, but we attribute this to experimental error. Equally, points in the de-amplified regime are attributed to experimental error or limits on resolution, especially in the regions where $V_T/V_S \approx 1$ and $V_S/V_T \approx 0$ (there is a 50 mV shift between the parametric and direct data which becomes relevant at those extremes).

Determining parametric advantage for the full nonlinear system is not analytically tractable, however, we demonstrate that parametric advantage remains unachievable by solving numerically Eq. 3 using the experimentally fitted parameters. To show why parametric advantage does not arise in the case of nonlinear MEMS devices despite the Duffing caused detuning, Fig. 4(a) shows simulated traces for the directly and parametrically driven 250 μm device and their ratio η obtained for $V_{dc} = 10$ V and an $V_T = 1$ and 300 mV. Fig. 4(a) shows that at low voltages, parametric pumping plays a negligible role and therefore the signal budget is better spent on directly driving the system. The value of η simply reduces to V_S/V_T for the linear case, while a peak in the case of strong drive is visible. This peak can be attributed to Duffing-caused detuning

of the resonance peak (the direct and parametric cases are unequally detuned according to Eq. 3). Even with this peak the value of η does not surpasses 1. A more detailed calculation is shown in Fig. 4(b) which shows a 2-dimensional plot of the maximum of η calculated numerically for the 250 μm device for $V_{dc} = 10$ V as a function of V_D and V_P normalized to the threshold voltage of instability $V_{cr} = 3.24$ V. Figure 4(b) demonstrates no possibility for parametric advantage even when a MEMS is driven into the nonlinear regime.

In summary, this work compared the response of nonlinear M/NEMS devices to direct forcing and parametric amplification using a single-mode expansion. The work described theoretically and demonstrated experimentally the need for a quadratic nonlinear component in order for parametric amplification to take place. Furthermore, this work investigated the regions in parameter space where parametric amplification would be more efficient than direct drive. Surprisingly, such parametric advantage does not exist for linear nor nonlinear, Duffing-type, systems if one accounts for both the pump and the signal. If, on the other hand, either the signal or the pump voltages are not part of the overall budget then parametric advantage can be achieved.

See the supplementary material for a derivation of Eq. 2, threshold voltage (V_T), and η .

-
- [1] D. Rugar and P. Grütter, Mechanical parametric amplification and thermomechanical noise squeezing, *Physical Review Letters* **67**, 699 (1991).
 - [2] I. Mahboob and H. Yamaguchi, Bit storage and bit flip operations in an electromechanical oscillator, *Nature nanotechnology* **3**, 275 (2008).
 - [3] I. Mahboob and H. Yamaguchi, Piezoelectrically pumped parametric amplification and q enhancement in an electromechanical oscillator, *Applied Physics Letters* **92** (2008).
 - [4] M. Gonzalez and Y. Lee, A study on parametric amplification in a piezoelectric mems device, *Micromachines* **10**, 19 (2018).
 - [5] G. Prakash, A. Raman, J. Rhoads, and R. G. Reifenger, Parametric noise squeezing and parametric resonance of microcantilevers in air and liquid environments, *Review of Scientific Instruments* **83** (2012).
 - [6] K. L. Turner, S. A. Miller, P. G. Hartwell, N. C. MacDonald, S. H. Strogatz, and S. G. Adams, Five parametric resonances in a microelectromechanical system, *Nature* **396**, 149 (1998).
 - [7] D. W. Carr, S. Evoy, L. Sekaric, H. G. Craighead, and J. Parpia, Parametric amplification in a torsional microresonator, *Applied Physics Letters* **77**, 1545 (2000).
 - [8] R. Karabalin, S. Masmanidis, and M. Roukes, Efficient parametric amplification in high and very high frequency piezoelectric nanoelectromechanical systems, *Applied Physics Letters* **97** (2010).
 - [9] E. Collin, T. Moutonet, J.-S. Heron, O. Bourgeois, Y. M. Bunkov, and H. Godfrin, Nonlinear parametric amplification in a triport nanoelectromechanical device, *Physical Review B—Condensed Matter and Materials Physics* **84**, 054108 (2011).
 - [10] A. Eichler, J. Chaste, J. Moser, and A. Bachtold, Parametric amplification and self-oscillation in a nanotube mechanical resonator, *Nano letters* **11**, 2699 (2011).
 - [11] C. Yang, Y. Zhang, H. Lu, C. Zhang, F. Chen, Y. Yan, F. Xue, A. Eichler, and J. Moser, Symmetry breaking of large-amplitude parametric oscillations in a few-layer graphene nanomechanical resonator, *arXiv preprint arXiv:2502.18827* (2025).
 - [12] J. Pribošek and M. Eder, Parametric amplification of a resonant mems mirror with all-piezoelectric excitation, *Applied Physics Letters* **120** (2022).
 - [13] J. Kim, Y. Kawai, N. Inomata, and T. Ono, Parametrically driven resonant micro-mirror scanner with tunable springs, in *2013 IEEE 26th International Conference on Micro Electro Mechanical Systems (MEMS)* (IEEE, 2013) pp. 580–583.
 - [14] H. Wakamatsu, T. Ono, and M. Esashi, Parametrically amplified resonant sensor with pseudo-cooling effect, in *18th IEEE International Conference on Micro Electro Mechanical Systems, 2005. MEMS 2005.* (IEEE, 2005) pp. 343–346.
 - [15] O. Thomas, F. Mathieu, W. Mansfield, C. Huang, S. Trolhier-Mckinstry, and L. Nicu, Efficient parametric amplification in micro-resonators with integrated piezoelectric actuation and sensing capabilities, *Applied*

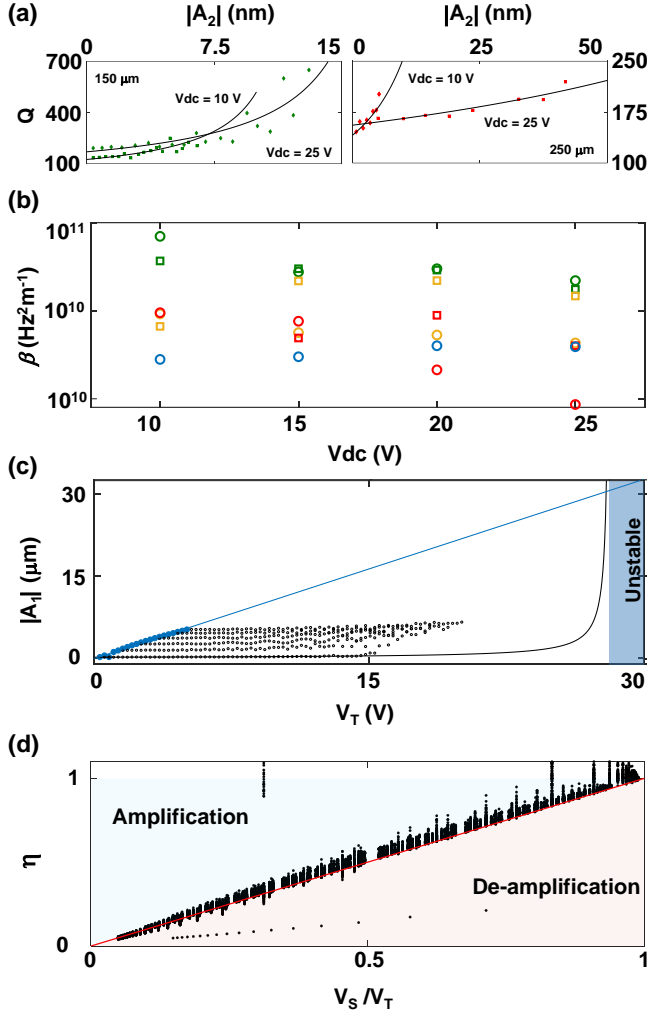


FIG. 3. Parametric amplification and quadratic nonlinearity. (a) Example fits of the quality factor versus the A_2 amplitude for the 150 μm and 250 μm devices for $V_{dc} = 10$ and 25 V. (b) Extracted β for all devices showing no strong dependence on dc voltage. (c) Comparison of direct (blue dots) and parametric (black dots) drives for the 150 μm device, for $V_{dc} = 10$ V. The plot demonstrates that upon extrapolation the direct drive (blue line) and parametric drive (black line) intersect practically at the onset of instability (blue shaded area). The x-axis is $V_T = V_D$ for the direct drive, and $V_T = V_S + V_P$ for the parametric case. (d) Plot showing the 150 μm experimentally measured ratio η as a function of the ratio V_S/V_T (black points), the red line indicates the $y = x$ diagonal, the red shaded area indicates de-amplification region, and the blue shaded area indicates amplification. The data points overwhelmingly fall below the $\eta = 1$ limit.

Physics Letters **102** (2013).

- [16] K. Harish, B. Gallacher, J. Burdess, and J. Neasham, Experimental investigation of parametric and externally forced motion in resonant mems sensors, *Journal of Micromechanics and Microengineering* **19**, 015021 (2008).
 [17] Y. Jia, J. Yan, K. Soga, and A. A. Seshia, Multi-frequency operation of a mems vibration energy harvester

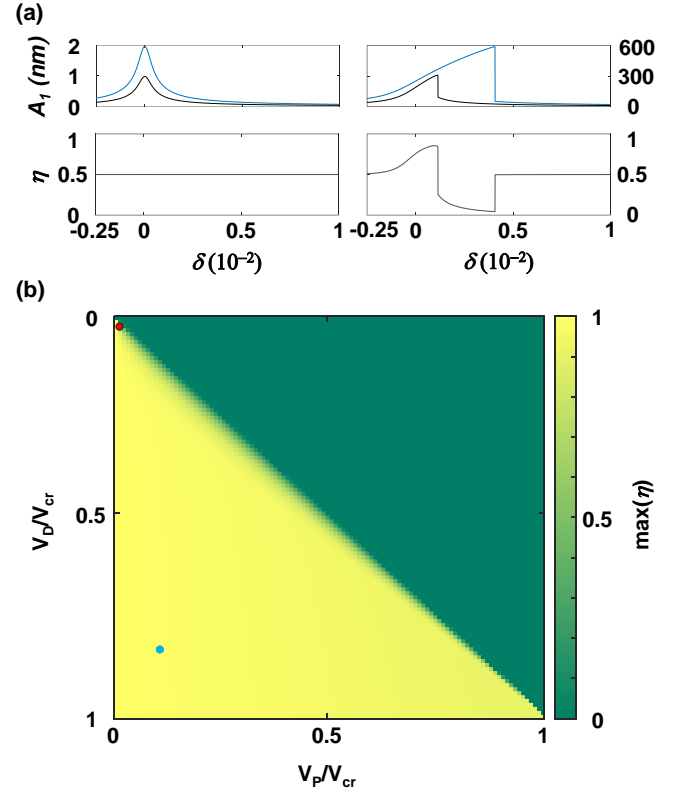


FIG. 4. Calculated η for the nonlinear case. (a) Two sets of traces for weak linear driving (left) and strong nonlinear driving (right) calculated using the device parameters of the 250 μm resonator. The linear case, calculated for $V_{dc} = 10$ V, $V_D = 1$ mV, $V_P = 0.5$ mV, and $V_S = 0.5$ mV, shows $\eta = 0.5$. For the nonlinear case, calculated for $V_{dc} = 10$ V, $V_D = 0.3$ V, $V_P = 0.15$, and $V_S = 0.15$ V, we see that due to detuning a peak in the value of η is obtained, although it does not cross the threshold of 1. (b) The maximum of η obtained for calculating all combinations of $V_P + V_S = V_T < V_{cr}$ for the device parameters corresponding to the 250 μm devices, showing no possibility of parametric advantage. The position in parameter space of the linear and nonlinear traces in (a) are shown as the red and blue dots, respectively.

by accessing five orders of parametric resonance, in *Journal of Physics: Conference Series*, Vol. 476 (IOP Publishing, 2013) p. 012126.

- [18] N. T. Beigh and D. Mallick, Highly efficient low threshold parametrically forced mems vibrational energy harvesters, in *2020 5th IEEE International Conference on Emerging Electronics (ICEE)* (IEEE, 2020) pp. 1–4.
 [19] H. Postma, I. Kozinsky, A. Husain, and M. Roukes, Dynamic range of nanotube-and nanowire-based electromechanical systems, *Applied Physics Letters* **86** (2005).
 [20] H. Westra, M. Poot, H. Van Der Zant, and W. Venstra, Nonlinear modal interactions in clamped-clamped mechanical resonators, *Physical review letters* **105**, 117205 (2010).
 [21] M. Aghamohammadi, V. Sorokin, and B. Mace, On the response attainable in nonlinear parametrically excited systems, *Applied Physics Letters* **115** (2019).
 [22] V. Kumar, J. K. Miller, and J. F. Rhoads, Nonlin-

- ear parametric amplification and attenuation in a base-excited cantilever beam, *Journal of sound and vibration* **330**, 5401 (2011).
- [23] J. F. Rhoads and S. W. Shaw, The impact of nonlinearity on degenerate parametric amplifiers, *Applied Physics Letters* **96** (2010).
- [24] B. Zaghari, E. Rustighi, and M. G. Tehrani, Dynamic response of a nonlinear parametrically excited system subject to harmonic base excitation, in *Journal of Physics: Conference Series*, Vol. 744 (IOP Publishing, 2016) p. 012125.
- [25] S. Neumeyer, V. Sorokin, and J. J. Thomsen, Effects of quadratic and cubic nonlinearities on a perfectly tuned parametric amplifier, *Journal of Sound and Vibration* **386**, 327 (2017).
- [26] M. Dykman, C. Maloney, V. Smelyanskiy, and M. Silverstein, Fluctuational phase-flip transitions in parametrically driven oscillators, *Physical Review E* **57**, 5202 (1998).
- [27] S. Houri, D. Hatanaka, M. Asano, and H. Yamaguchi, Demonstration of multiple internal resonances in a micro-electromechanical self-sustained oscillator, *Physical Review Applied* **13**, 014049 (2020).
- [28] S. Houri, M. Asano, H. Yamaguchi, N. Yoshimura, Y. Koike, and L. Minati, Generic rotating-frame-based approach to chaos generation in nonlinear micro-and nanoelectromechanical system resonators, *Physical Review Letters* **125**, 174301 (2020).
- [29] S. A. Emam and A. H. Nayfeh, On the nonlinear dynamics of a buckled beam subjected to a primary-resonance excitation, *Nonlinear Dynamics* **35**, 1 (2004).
- [30] M. I. Younis, *MEMS linear and nonlinear statics and dynamics*, Vol. 20 (Springer Science & Business Media, 2011).
- [31] A. N. Cleland, *Foundations of nanomechanics: from solid-state theory to device applications* (Springer Science & Business Media, 2013).
- [32] C. Fragkiadakis, S. Sivaramakrishnan, T. Schmitz-Kempen, P. Mardilovich, and S. Trolier-McKinstry, Heat generation in pzt mems actuator arrays, *Applied Physics Letters* **121** (2022).